1987ApJ...317..290C

THE ASTROPHYSICAL JOURNAL, 317:290–302, 1987 June 1
© 1987. The American Astronomical Society. All rights reserved. Printed in U.S.A.

POLARIZATION OF LIGHT SCATTERED FROM THE WINDS OF EARLY-TYPE STARS

J. P. CASSINELLI
Astronomy Department, University of Wisconsin, Madison, and Sonnenborgh Observatory
AND
K. H. NORDSIECK AND M. A. MURISON
Astronomy Department, University of Wisconsin, Madison
Received 1986 June 2; accepted 1986 November 11

ABSTRACT

There is evidence from visible wavelength polarimetry that the matter in the winds of early-type stars is not distributed uniformly about the stars. It is becoming possible to measure polarization with high precision in the ultraviolet from orbiting telescopes. With these observations, details of the spatial distribution of the mass loss may be studied. In this paper equations for the observable polarization from an axisymmetric distribution of electrons are derived first from the basic point source model of Brown and McLean and then from extended atmosphere radiative transfer theory. A factor is derived which corrects the Brown and McLean model for the finite size of stars. This finite disk factor is found to reduce the magnitude of the predicted polarization to less than half of the point source prediction. Another correction factor, not considered in this paper, would be required for cases in which part of the electron scattering envelope is occulted by the star. We consider the effects of having the mass outflow concentrated in a plume. The effects of absorption in an unocculted plume are shown to give rise to a wavelength-dependent polarization that is described using a "polarization color" parameter. A continuum opacity index is defined that allows for a straightforward interpretation of the polarization of stars of differing effective temperatures. An attempt is made throughout to isolate the dominant geometrical factors, plume parameters, and absorption properties that affect the observable polarization.

Subject headings: polarization — radiative transfer — stars: early-type — stars: winds

I. INTRODUCTION

During the past 15 years spectropolarimetry has been developing into a powerful new approach to study the spatial structure of the stellar atmospheres and stellar winds of early-type stars. Pioneering observations by Serkowski (1970) indicated that several classes of early-type stars show intrinsic polarization of as much as 1% or 2% in the net flux from the star. This is significantly larger than expected from plane-parallel model atmospheres for rotationally distorted stars (Collins 1972) but could be explained by asymmetries in very extended atmospheres (Cassinelli and Hummer 1971). In an extended atmosphere the radiation field is peaked strongly in the outward direction and leads to highly polarized line-of-sight intensities, such as the $\sim 50\%$ polarization of the light scattered in the solar corona. In the case of a distant star, one measures the radiation integrated over the full disk of the star, and the large polarization in one quadrant of the disk tends to be cancelled out by the polarization from the adjacent quadrant. The intrinsic polarization seen in the net flux in some stars means, therefore, that there is a substantial asymmetry in the geometry of their extended atmospheres or winds.

The ability of polarization measurements to diagnose distortions and asymmetries of stellar winds has greatly increased the interest in the subject of spectropolarimetry. Asymmetry in winds can be caused by magnetic structures in the atmospheres of hot stars, by rotation, and perhaps by nonradial pulsations of their interior structure. There is an increasingly convincing body of evidence that hot stars may have open and closed magnetic structures in their atmospheres similar to the coronal holes and neighboring closed regions in the outer solar atmosphere (Underhill 1984; Cassinelli 1985). On the basis of X-ray line emission at 2.2 keV, Cassinelli and Swank (1983) have argued that there are confined regions with $T \geq 15 \times 10^6$ K in OB supergiants. Variability and sharp absorption components has been interpreted as evidence for variations in the mass outflow flux across the face of early-type stars (Underhill 1984; Mullan 1984). For helium-rich stars that have measured kilogauss magnetic fields, there is clear evidence from ultraviolet spectral lines that the mass flows out in plumes in the open field regions (Barker *et al.* 1982; Brown, Shore, and Sonneborn 1985). The random variability of the position angle of optical polarization in OB supergiants also suggests that the outflow occurs from several plumes in OB supergiants (Lupie and Nordsieck 1987). Cassinelli (1985) summarizes the evidence from observations at essentially all wavelengths that mass loss from hot stars is not isotropic. The spatial concentration of mass loss may be produced by magnetic fields, but it may also be related to the nonradial pulsation that is observed to occur in early-type stars (Vogt and Penrod 1983).

It is becoming possible to measure the polarization of stars to very high accuracy at ultraviolet wavelengths using the spectropolarimeters on NASA's Shuttle-launched Astro mission and on several Space Telescope instruments. The Wisconsin ultraviolet photo-polarimeter experiment (WUPPE) on the Astro mission can measure continuum polarizations to sensitivities of a few hundredths of a percent in the wavelength region 1400–3200 Å.

Because of the interest in asymmetric winds and the new capability of measuring the polarization of material in the winds with space experiments, we choose to focus on ultraviolet polarization caused by mass outflow concentrated in plumes. A straightfor-

© American Astronomical Society • Provided by the NASA Astrophysics Data System

1987ApJ...317..290C

ward method has been developed by Brown and McLean (1977) for computing polarization from any axisymmetric electron-scattering envelope about a point source star. In § II, we reconsider the equations of Brown and McLean for axisymmetric distributions of electrons, and develop a factor to correct for the finite size of a star. In § III we specifically consider the geometry of a plume and discuss the frequency dependence of the polarization that arises because of absorptive opacity in the plume. In § IV numerical results of model calculations are presented, and these are shown to lead to useful diagrams for diagnosing the structure of plumes in stars which have different effective temperatures and plume mass-loss rates.

II. POLARIZATION PRODUCED BY AXISYMMETRIC ELECTRON ENVELOPES

The majority of the papers on polarization in hot stars have focused on the effects of rotationally distorted envelopes. This is because of the rather large polarization observed in rapidly rotating Be stars. Collins (1972) and Haisch and Cassinelli (1976) used radiation transfer methods to derive the polarization that can arise in the outer layers of atmospheres that are rotationally distorted. Their methods could treat tranfer in both optically thick and thin media. However, the ability to treat optically thick situations is not of prime interest because the polarization caused by electron scattering tends to be negated if secondary scatterings occur. The much simpler case of polarization in an optically thin equatorial disk or ring about a point source was treated by Shakhovskoi (1965) and Capps, Coyne, and Dyck (1973). The restriction to equatorial models was lifted by Brown and McLean (1977), who derived the equations for any axisymmetric distribution of electrons about a point source. Their method will be a starting point for our analysis. We also show that the radiation transfer methods are compatible with the optically thin point source analysis of Brown and McLean, and can be used in a straightforward way to allow for the effects of the finite size of the star. The inclusion of a finite disk factor reduces the predicted polarization considerably.

a) The Point Source Case

Let us consider a point source at 0 at the center of a set of axes, (x, y, z), with $0z$ along the axis of rotational symmetry (hereafter called the polar axis) and with $0y$ in the plane of the sky (see Fig. 1). The (x, y, z) set of axes is associated with a star-centered spherical coordinate system (r, θ, ϕ), with r being the radial distance to the point of interest E, θ being the polar angle from the z-axis to the r-direction, and ϕ being the azimuthal angle. Consider also an observer-oriented frame of reference (X, Y, Z) that is also centered on 0, but with the $0Z$ azis in the direction toward the observer and the Y axis along y. The angle between the polar axis z and the Z axis is the inclination angle i. It is convenient to define two other coordinate systems related to the (X, Y, Z) observer-oriented frame. Let (r, χ, ϕ) be spherical coordinates of the point E relative to the $(X, Y, Z$ frame), where χ is the polar angle, and, as is seen in Figure 1, χ is the angle through which light is scattered toward the observer. The angle ϕ is the azimuthal angle in the XY plane (the plane of the sky). Finally, since we will be considering radiative transfer along various lines of sight through the electron envelope, it is convenient to define the standard coordinates used in extended stellar atmosphere theory (Hummer and Rybicki 1971; Cassinelli and Hummer 1971). Let (p, ϕ, Z) be the cylindrical coordinates of the point E, where p is the "impact parameter" of the line of sight to the star and ϕ and Z are the azimuthal angle and the distance along the line of sight rectangular coordinate, respectively, as defined earlier.

Electrons at a point E in the envelope scatter light through an angle χ toward the observer (see Fig. 1). The electrons are induced to oscillate perpendicular to the radius vector $\boldsymbol{r}$, and the observed light is polarized in a direction that is parallel to the vector $d\boldsymbol{\phi}$. Consider the electrons in the volume element $dV = r^2 \sin \theta d\theta d\phi dr$. The intensity of the light scattered toward the observer is

$$dI_\nu = \frac{L_\nu}{4\pi r^2}\left(\frac{s}{4\pi}\right) n_e(r, \theta, \phi)\, \frac{3}{4}\,(1 + \cos^2 \chi) dV \,, \tag{1}$$

where L_ν is the monochromatic stellar luminosity, s is the Thompson cross section, n_e is the electron density, and $3(1 + \cos^2 \chi)/4$ is the Rayleigh scattering phase function. This scattered radiation is polarized as measured by the observer. Let $I(X)$ be the intensity measured through a filter that transmits light which has its electric vector parallel to the X-axis, and let $I(Y)$ be the corresponding intensity measured parallel to the Y-axis. The polarization is described using the second Stokes parameter $I_\nu^Q = I_\nu(Y) - I_\nu(X)$. The third Stokes parameter I_ν^U is a similar difference in intensities but relative to a set of observer coordinates X', Y' that are formed by a rotation of 45° about the $0Z$ direction. The Stokes parameters associated with the scattering from the volume of electrons dV are

$$\left.\begin{matrix} dI_\nu^Q \\ dI_\nu^U \end{matrix}\right\} = \frac{L_\nu s n_e(r, \theta, \phi) dV}{(4\pi r)^2} \left\{\begin{matrix} \frac{3}{4}\,(\sin^2 \chi \cos 2\phi) \\ \frac{3}{4}\,(\sin^2 \chi \sin 2\phi) \end{matrix}\right. \tag{2}$$

Brown and McLean (1977) show that a transformation from the ϕ, χ observer-oriented coordinates to the θ, ϕ star-centered coordinates allows one to derive the polarization from a general axisymmetric distribution of electrons. The transformations appropriate for the coordinates shown in Figure 1 are

$$\cos \chi = \cos \theta \cos i + \sin \theta \cos \phi \sin i \,, \tag{3}$$

$$\sin \chi \cos \phi = \sin \theta \cos \phi \cos i - \cos \theta \sin i \,, \tag{4}$$

$$\sin \chi \sin \phi = \sin \theta \sin \phi \,. \tag{5}$$

Let us use these relations in equation (2). Since we are interested in an axisymmetric distribution, we integrate over ϕ from 0 to 2π.

© American Astronomical Society • Provided by the NASA Astrophysics Data System

1987ApJ...317..290C

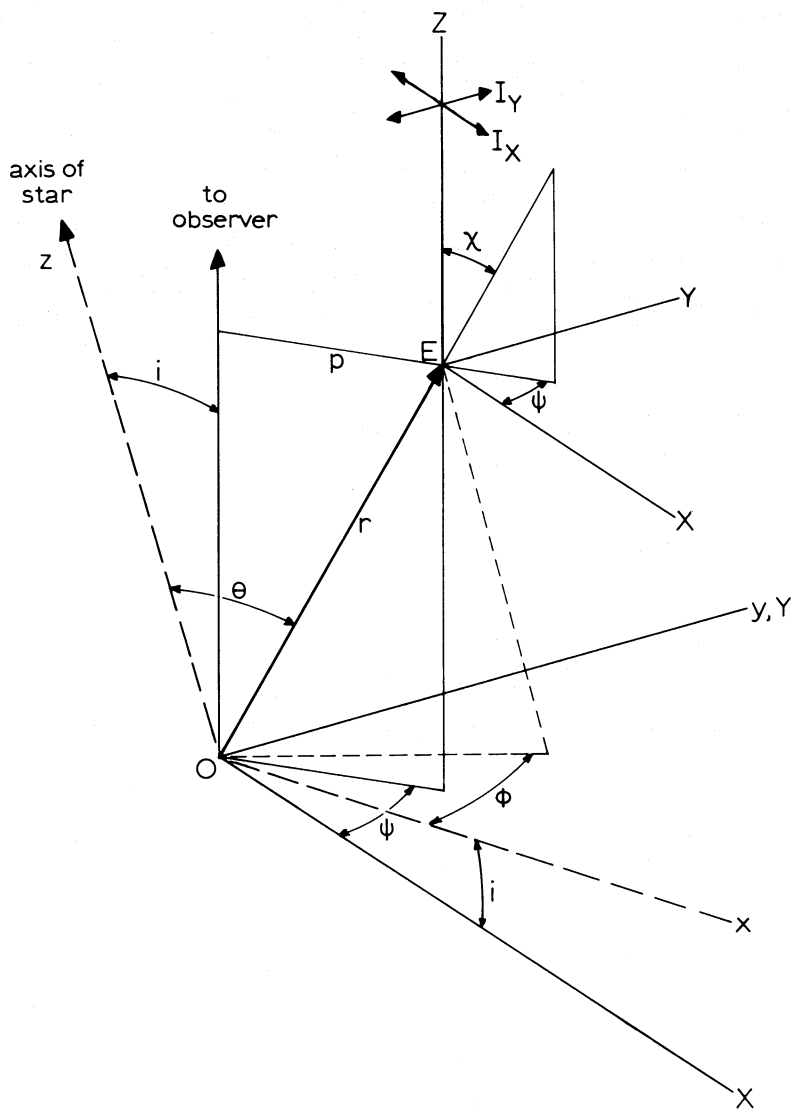

FIG. 1.—Star-centered $(x, y, z,)$ and observer-sky (X, Y, Z) coordinate systems used in the description of the scattering of polarized light. They X-Y plane is in the plane of the sky, z is along the rotation axis of the star, the observer is at inclination angle i, and the photon source is at the origin 0. Light scatters off an electron at P through an angle χ toward the observer and is linearly polarized parallel to an increment of the angle ϕ which is measured in the sky plane from the X-axis.

Consider the I_ν^Q case for example. We find

$$\int_0^{2\pi} (\sin^2 \chi \cos 2\phi) d\phi = \int_0^{2\pi} (1 - \cos^2 \chi)(1 - 2 \sin^2 \phi) d\phi = -\pi \sin^2 i(1 - 3\mu^2) , \tag{6}$$

where $\mu = \cos \theta$. Thus, the polarized integrated intensity over the volume containing electrons is

$$Q_\nu = \int \frac{dI_\nu^Q}{dV} dV = -\frac{\pi L_\nu}{(4\pi)^2} \left(\frac{3}{4} s\right) \sin^2 i \int_r \int_\mu (1 - 3\mu^2) n_e(r, \mu) d\mu dr , \tag{7}$$

and

$$U_\nu = \int \frac{dI_\nu^U}{dV} dV = 0 ,$$

(because of our choice for the direction of the Y-axis). A similar integration over dI_ν in equation (1) would give the enhancement of the brightness of the star caused by light that is scattered by the electron envelope toward the observer,

$$\Delta L_\nu = 4\pi \int \frac{dI_\nu}{dV} dV .$$

© American Astronomical Society • Provided by the NASA Astrophysics Data System

1987ApJ...317..290C

This is small for the cases of interest in this paper, and we simply represent ΔL_ν as a fraction, δ, of L_ν, so that $L_\nu(\text{total}) = L_\nu(1 + \delta)$. For the case of coherent electron scattering δ is independent of frequency, but we can allow for a contribution by frequency-dependent emission from the envelope ΔL_ν^{em}, in which case δ is a function of frequency.

The "net polarization" is defined by

$$P_\nu = \frac{4\pi Q_\nu}{L_\nu(1 + \delta_\nu)}, \tag{8}$$

since $U_\nu = 0$. The net polarization is usually expressed as a percentage of polarization.

b) The Finite Star Case

The observable polarization depends not only on the distribution of electrons and the aspect angle i, but also on the anisotropy of the incident radiation field. This was discussed in some detail by Cassinelli and Hummer (1971) in their paper on the transfer of polarized light through an extended stellar atmosphere. The anisotropy of the incident radiation is there called the "forward peaking" of the radiation field. At the surface of a star that is assumed to be the uniform disk (i.e., with no limb darkening) the outward radiation is isotropic over the outward half-hemisphere. For the electrons in this radiation field there would be no preferential direction for the oscillations that are induced on scattering of the radiation field. The contribution to polarization by electrons in this radiation field would be zero. Far from this star of radius R_*, radiation would be strongly peaked in the outward radial direction. The intensity along a line of sight at large impact parameters, $p \gg R_*$, tends to be highly polarized (greater than 50%). Based on these results from extended atmosphere theory, we should expect that the polarization derived by assuming that the central source is a point will be far too large, since the light from a point source is strongly peaked in the outward direction at all positions in the atmosphere.

Here we use a simplified version of the transfer equation approach of Cassinelli and Hummer (1971) to reanalyze the polarization expected from an optically thin, axisymmetric distribution of electrons. For convenience we drop the subscript, ν, but the results are valid for monochromatic radiation. Consider a line of sight at an impact parameter, p, that intersects the electron envelope. Following Chandrasekhar (1950), let I_L and I_R be the intensities parallel and perpendicular, respectively, to the plane containing the radius vector and the line of sight. Relative to the center of the star I_L is the radial component of intensity and I_R is the tangential component. The respective source functions are

$$S_L = \tfrac{3}{4}[2(J_L - K_L) + \cos^2\chi(3K_L - 2J_L + J_R)], \tag{9}$$

and

$$S_R = \tfrac{3}{4}(J_R + K_L), \tag{10}$$

where J and K are, respectively, the mean intensity and second moment of the radiation field at r, and χ is the scattering angle, shown in Figure 1.

There are several simplifications that apply to the optically thin problem. The radiation field at r is dominated by the direct radiation field of the star. The diffuse component arising from scattering elsewhere in the envelope is small. The direct stellar radiation is unpolarized because the central star can be assumed to be spherically symmetric. Thus, $J_R = J_L = \frac{1}{2}J$, $K_R = K_L = \frac{1}{2}K$, and similarly for the first moment of the intensity that is related to the flux, $H_R = H_L = \frac{1}{2}L/(4\pi r)^2$. The line-of-sight intensities are, for the optically thin case,

$$I_L = \int S_L\, d\tau_Z = \int_{-\infty}^{+\infty} S_L n_e s dZ, \tag{11}$$

and

$$I_R = \int_{-\infty}^{+\infty} S_R n_e s\, dZ, \tag{12}$$

and the difference in the two intensities is, with the approximations above,

$$I_R - I_L = \int_{-\infty}^{+\infty} (S_R - S_L) n_e s dZ = \int_{-\infty}^{+\infty} \tfrac{3}{4}(3K_L - J_L)(1 - \cos^2\chi) n_e s\, dZ. \tag{13}$$

Relative to the X and Y axes, the polarized intensities are

$$I^Q = I(Y) - I(X) = (I_R - I_L)\cos 2\phi, \tag{14}$$

$$I^U = (I_R - I_L)\sin 2\phi. \tag{15}$$

We now integrate over the projected area of the envelope on the X, Y plane to get the total polarization

$$Q = \iiint \tfrac{3}{4}(3K_L - J_L) n_e s \sin^2\chi \cos 2\phi dX dY dZ. \tag{16}$$

Transforming the volume element to star-centered coordinates, we have inside the integral $dXdYdZ = dxdydz = r^2 \sin\theta d\theta d\phi$. The

© American Astronomical Society • Provided by the NASA Astrophysics Data System

1987ApJ...317..290C

electron envelope is axisymmetric, so we may carry out the integral over ϕ as we did in equation (6) and get

$$Q = -(\tfrac{3}{4}s)\pi \sin^2 i \int_r \int_\mu n_e r^2 (3K_L - J_L)(1 - 3\mu^2) d\mu dr \,, \tag{17}$$

where K_L and J_L are functions of radius alone.

Consider the point source asymptotic limit: if the radiation field is radial, i.e., strongly peaked in the forward direction, the moments of the radiation field become identical; $J = H = K$. Therefore $(3K_L - J_L) = L/(4\pi r)^2$, and equation (17) reduces exactly to equation (7). This suggests thay we can define a correction factor to the point source result that accounts for the effect of a finite disk.

On comparing equation (17) and (7), we define a finite disk correction factor to be the ratio of the polarization expected from a source with a finite disk to that of a point source. This is

$$D \equiv \frac{3K - J}{2H} = \frac{(4\pi r)^2}{L} \frac{1}{4} \int_{\mu_*}^{1} I_* (3\mu^2 - 1) d\mu \,, \tag{18}$$

where $\mu = \cos\theta$, θ_* is the angular radius of the star, as seen from r, and I_* is the intensity from the stellar surface, which for a uniform disk is $\pi I_* = L/(4\pi R_*^2)$. This gives finally

$$D(r) = (1 - R_*^2/r^2)^{1/2} \tag{19}$$

as the finite disk depolarization factor. The factor $D(r)$ rises from zero at $r = R_*$ to unity at large radius. It accounts for the fact that the contribution to the polarization from regions very near the star is small because of the small forward peaking of the radiation field.

There is another effect associated with a star with a finite disk. The disk occults from the line of sight the region on the far side of the star, and therefore blocks the radiation scattered toward the observer from that region. This is a problem that, of course, does not arise in the point source case. The only aspect angle factor that occurs for the point source case is the $\sin^2 i$ factor in equation (8). This factor is adequate for the finite disk case only so long as a small fraction of the electrons in the envelope are occulted. A proper analysis of the occultation effect will require line-of-sight integrations over the disk area. This will not be done in the present paper. However, we should note that radiation scattered from electrons which are directly in front and behind the star is unpolarized; the scattering angle χ being 0° or 180° (see eq. [2]). Thus the polarization from the occulted material might not be very large.

To conclude this section, we can write the net polarization for an optically thin axisymmetric distribution of electrons including the effect of the correction factor D for the finite size of the star. Combining equations (7), (8), and (19), the net polarization $P = Q/(L/4\pi)$ is

$$P_\nu = -\left[\frac{3s \sin^2 i}{16(1 + \delta_\nu)}\right] \int_r \int_\mu (1 - 3\mu^2) D(r) n_e(r, \mu) d\mu dr \,. \tag{20}$$

This expression is valid for a rotationally distorted equatorial envelope as well as for polar plumes or jets. In the next section we consider plume gometries. Friend and Cassinelli (1986) have applied equation (20) to a consideration of the focused wind in Cygnus X-1, and Waters and Cassinelli (1987) have applied the equation to the rotationally distorted outflows from Be stars.

III. POLARIZATION FROM A PLUME OF ELECTRONS

a) Polarization per Unit Solid Angle

Brown and McLean (1977) discuss several axisymmetric distributions of electrons for which the r and μ integrals clearly separate into simple column density integrals and "shape factors." In the case in which the electrons are confined to a cone or "plume" centrally aligned with the polar z-axis one has

$$n_e(r, \theta) = \begin{cases} n_e(r) & 0 < \theta < \theta_p \quad \text{or} \quad \mu_p < \mu < 1 \,, \\ 0 & \theta_p < \theta \quad \text{or} \quad \mu < \mu_p \,, \end{cases} \tag{21}$$

where θ_p is the plume opening angle and $\mu_p = \cos\theta_p$. The angular integral that appears in equation (20) or "shape factor" is

$$G(\mu_p) \equiv \int_{\mu_p}^{1} (1 - 3\mu^2) d\mu = \mu_p^3 - \mu_p = -\frac{\Omega_p}{\pi} + \frac{3}{4}\left(\frac{\Omega_p}{\pi}\right)^2 - \frac{1}{8}\left(\frac{\Omega_p}{\pi}\right)^3 \,, \tag{22}$$

where $\Omega_p = 2\pi(1 - \mu_p)$ is the plume solid angle. This expression for G indicates the following: for a plume with a given density profile $n_e(r)$ and with a narrow opening angle, the polarization depends linearly on the solid angle, Ω_p, because the total number of scattering electrons increases with Ω_p. When Ω_p becomes large (≥ 1), the polarization reaches an extremum at $\mu_p = 3^{-1/2}$ (which corresponds to $\theta_p = 54\overset{\circ}{.}7$, $\Omega_p = 2.65$ sr), and then decreases in magnitude because the polarization from electrons on one side of the plume partially cancels that from electrons on the other side of the plume. The polarization *per electron* ($\propto G/\Omega_p$) is relatively constant for a narrow plume and drops sharply for solid angles larger than ~ 1 sr. We will confine our discussion to narrow plumes. For narrow plumes, it is convenient to refer to the polarization per unit solid angle, which we shall designate as

$$\tilde{P} = \frac{dP}{d\Omega} \,.$$

© American Astronomical Society • Provided by the NASA Astrophysics Data System

1987ApJ...317..290C

Combining equations (20) and (22), we find in the narrow plume limit,

$$\tilde{P}_\nu = \left[\frac{3s \sin^2 i}{16\pi(1+\delta_\nu)}\right] \int_{R_*}^{\infty} n_e(r) D(r) dr \ . \tag{24}$$

This is the polarization per unit solid angle of a narrow plume observed at an inclination angle i, corrected for the nonradial radiation field of a disk. We note that the maximal polarization for a given $n_e(r)$, attained at $\Omega_p = 2.65$ sr, as noted above, is related to $\tilde{P}$ through $P_{\max} = 1.21\tilde{P}$.

As mentioned above, the finite photospheric disk of the star will occult from the observer the electrons that are behind the star. Since we are not here accounting for this effect, equation (24) is not valid for large plume inclination angles, say, from $i = 150°$ to $i = 180°$ (depending on the radial distribution of the electrons). The equation is accurate for plumes in the plane of the sky, $i \approx 90°$. In this orientation $\sin^2 i = 1$, and the polarization has its largest value. The equation is also valid for plumes extending toward the observer ($i = 0°$), in which case we expect no net polarization because the relevant scattering is symmetrical about the forward direction.

From equation (24), one would conclude that almost no wavelength dependence of the polarization is expected because L_ν has cancelled in converting to net polarization. The only frequency-dependent term in equation (24) is the small quantity δ_ν. This is shown with a frequency subscript only because there could be, say, frequency dependent thermal emission that would enhance the flux from the envelope at certain wavelengths. In the next section we discuss a more important source of frequency-dependent polarization: absorption occurring in the plume.

b) Frequency-dependent Absorption Effects

McLean (1979) discusses in a general way the effects of frequency-dependent absorption within the envelope and absorption between the envelope and the observer. We will focus only on the absorption that occurs along the plume from the star and assume there is no absorption once the photon is scattered. We will ignore absorption of the direct starlight that might occur because of material outside the plume. Absorptive opacity within the plume gives rise to frequency dependence of the polarization because at frequencies where the absorptive opacity, κ_ν, is larger, a smaller fraction of the stellar monochromatic luminosity reaches the scattering electrons. The thermal emission that is the inverse of the absorption process, represented by the term δ_ν in equation (24), also give rise to a frequency dependence which will be ignored here. These approximations are satisfied for a thin plume that contains most of the outflowing material.

We can find the maximum effect of the absorption in the plume by attenuating the photospheric emission by a factor $e^{-\tau_\nu}$, where τ_ν is the absorption along the column from R_* to the scattering point r. Using this column is the same as assuming that the stellar radiation field is radial, so that there is no radiation incident on the plume from the limb of the photosphere. Accounting for the radiation along all rays from r that intercept a point on the photosphere would be a calculation as difficult as accounting for the occultation effects of a finite disk, and we choose to defer such detailed analyses for a later paper.

Replacing L_ν^* with $L_\nu^* e^{-\tau_\nu(r)}$ in equation (20) and hence also in equation (24), we get for the polarization per unit solid angle in the limit of narrow plumes

$$\tilde{P}_\nu = \left[\frac{3s \sin^2 i}{16\pi(1+\delta_\nu)}\right] \int_{R_*}^{\infty} n_e(r) e^{-\tau_\nu(r)} D(r) dr \ . \tag{25}$$

In § IV, we describe numerical solutions of equation (25) accounting for wavelength-dependent opacity in a plume. But, first, let us consider a simplified model that will allow us to isolate the important parameters that determine the wavelength dependence of a star's polarization.

c) The "Color" for the Polarization: Definition and a Simplified Model

Let us define the "color" C of the polarization as the normalized difference in polarization at two continuum frequencies, ν_A and ν_B:

$$C \equiv \frac{P(\nu_A) - P(\nu_B)}{P(\nu_A)} \ . \tag{26}$$

In such a ratio, the factors that are common to the polarization at both frequencies cancel out. Thus, color is independent of $\sin^2 i$ and of the geometry factor G. In our plume problem this means C is independent of the plume-opening angle. By considering a simplified model we show that C has a different dependence on the density distribution in the envelope than does the monochromatic polarization $P(\nu)$. The color depends on an integral over the square of the electron density, while the monochromatic polarization depends on the linear column density through the envelope. The numerical results of the next section will show that our simplified derivation gives basically the correct trend and confirms that interesting new information can be derived from the color of the polarization.

The main reason that there is a frequency dependence of the intrinsic polarization is because of the absorption of stellar light in the plume. The optical depth τ_ν in equation (25) is composed of an electron-scattering part, τ^{sc}, and an absorption optical depth τ_ν^{AB}. To isolate the absorption part, let us consider the quasi-optically thin case, in which we may write

$$e^{-\tau_\nu(r)} \approx 1 - \tau^{sc}(r) - \tau^{AB}(\nu, r) \ . \tag{27}$$

Let us consider the ultraviolet frequencies where the dominant absorptive opacity is bound-free opacity from the $n = 2$ level of

© American Astronomical Society • Provided by the NASA Astrophysics Data System

1987ApJ...317..290C

hydrogen. The absorption optical depth is

$$\tau^{\mathrm{AB}}(\nu, r) = \int_{R_*}^{r} \kappa_\nu \rho dr = \int_{R_*}^{r} n_2 a_2(\nu) dr , \tag{28}$$

where $a_2(\nu)$ is the frequency-dependent cross section in the Balmer continuum that is commonly approximated by

$$a_2(\nu) = a_0 \nu_0^3/\nu^3 , \tag{29}$$

where ν_0 is the Balmer edge frequency (at $\lambda_0 = 3646$ Å), and n_2 is the population of the $n = 2$ level. The value of n_2 depends on the radiation field at r and on the electron density $n_e(r)$. Let us separate two factors in a rough way by assuming that the $n = 2$ population is determined by statistical balance between photoionization and radiative recombination (and cascade). Therefore,

$$n_2 = n_p n_e \alpha_2 \Big/ \int_{\nu_0}^{\infty} \frac{4\pi}{h\nu} a_\nu J_\nu d\nu , \tag{30}$$

$$\approx n_e^2 \alpha_2 \Big/ \int_{\nu_0}^{\infty} \frac{4\pi}{h\nu} a_\nu W B_\nu(T_{\mathrm{eff}}) d\nu , \tag{31}$$

$$\equiv n_e^2 q_2(r, T_{\mathrm{eff}}) , \tag{32}$$

where we have assumed that the proton density equals the electron density and that the mean intensity is spatially diluted radiation from a photosphere with a Planckian distribution with a temperature equal to the effective temperature, and α_2 is the recombination coefficient to the $n = 2$ level. This expression isolates the n_e^2 dependence of the $n = 2$ population and hence of the absorptive opacity and of the absorptive column density. Using equation (20), we can write the difference in the polarization at two wavelengths, as

$$P(\nu_A) - P(\nu_B) = \tfrac{3}{16} \sin^2 i \; G \int_{R_*}^{\infty} D(r)[\tau^{\mathrm{AB}}(\nu_B, r) - \tau^{\mathrm{AB}}(\nu_A r) n_a s dr , \tag{34}$$

where G and D are the envelope geometry and finite star depolarization factors introduced above. The difference in absorption optical depth separates into a frequency factor and an emission measure integral. The color C is given approximately by

$$C \approx a_0 \nu_0^3 \left(\frac{1}{\nu_B^3} - \frac{1}{\nu_A^3}\right) \int_{R_*}^{\infty} D(r) \int_{R_*}^{r} n_e^2 q(r', T_{\mathrm{eff}}) dr' n_e s dr \Big/ \int_{R_*}^{\infty} D(r) n_e s dr . \tag{35}$$

In this we see that there is no dependence on $\sin^2 i$ or on the plume-opening angle. There remains a rather complicated dependence on the density structure. However, we can note that if $n_e(r)$ is determined by a scaling constant such as the mass flux constant, $\dot{M}$, then there is a net dependence of the color on $\dot{M}^2$, while the monochromatic polarization depends linearly on $\dot{M}$.

In describing the color of the polarization, we find it useful to isolate the effective temperature dependence from the electron density dependence, and we use the average value of q_2 defined by

$$\bar{q}_2(T_{\mathrm{eff}}) = \int_{R_*}^{\infty} n_2 dr \Big/ \int_{R_*}^{\infty} n_e^2 dr , \tag{36}$$

$$\bar{q}_2(T_{\mathrm{eff}}) = \int_{R_*}^{\infty} q_2(r, T_{\mathrm{eff}}) n_e^2 dr \Big/ \int_{R_*}^{\infty} n_e^2 dr . \tag{37}$$

The simplified model discussed in this section has allowed us to note that the color and monochromatic polarizations depend differently on the density distribution, and we can partially isolate the frequency temperature and density dependences of the color of the polarization.

IV. MODEL RESULTS

We have chosen to consider the physical problem in which the polarization of a star is caused by enhanced mass loss along a plume. The plume is defined geometrically by the opening angle θ_p and aspect angle i. The density distribution along the plume can be described by specifying a wind velocity law along with the mass-loss rate. Because values for stellar mass-loss rates of early-type stars are familiar to many readers, we choose to use as a parameter the mass-loss rate the star would have if the plume extended over the full surface of the star:

$$\dot{M} = 4\pi\rho(r) v(r) r^2 . \tag{38}$$

Thus the actual mass-loss rate in the plume of solid angle $\Delta\Omega$ is

$$\Delta\dot{M} = \dot{M}\Delta\Omega/4\pi . \tag{39}$$

For the velocity distribution along the plume, $v(r)$, we use the velocity law expected from radiatively driven wind theory and used by Cassinelli and Olson (1979),

$$v^2(r) = v_0^2 + v_1^2(1 - R_*/r) , \tag{40}$$

which has a terminal velocity v_∞ given by $v_\infty^2 = v_0^2 + v_1^2$. We specify v_∞, and we let $v_0 = 0.1 v_\infty$, as a rough estimate of the velocity at which there is a significant contrast between the density in and out of the plume.

© American Astronomical Society • Provided by the NASA Astrophysics Data System

1987ApJ...317..290C

A quantity that is especially useful for describing the amount of scattering material is the electron scattering optical depth radially along the plume, τ_{es}:

$$\tau_{es} = \int_{R_*}^{\infty} n_e s dr \,, \tag{41}$$

or, equivalently,

$$\tau_{es} = \int_{R_*}^{\infty} \sigma_{es} \rho dr \,, \tag{42}$$

where $\sigma_{es} = s/(\mu_e m_H)$ with $\mu_e m_H$ being the mean mass of the outflowing particles per electron and σ_{es} is the electron scattering opacity per gram, which is for a pure fully ionized hydrogen gas, 0.4 $cm^2\ g^{-1}$. The integral in equation (42) is carried out using $2vdv = v_1^2 R_* dr/r^2$, yielding

$$\tau_{es} = \frac{\sigma_{es} \dot{M}}{2\pi(v_\infty + v_0)R_*} \,. \tag{43}$$

Thus the mass-loss parameter, $\dot{M}$, also directly gives the plume optical depth. For our numerical calculations we have chosen to use $R_* = 30\ R_\odot$ and $v_\infty = 2000\ km\ s^{-1}$.

To compute the wavelength-dependent hydrogen opacity, κ_ν, we need the populations of the hydrogen in the plume. We have chosen to estimate these using the Sobolev method (Castor 1970) that was employed by Cassinelli, Olson, and Stalio (1978) for deriving Hα line profiles from stellar winds. The collisional rates are computed assuming an electron temperature of $0.9T_{eff}$, and the

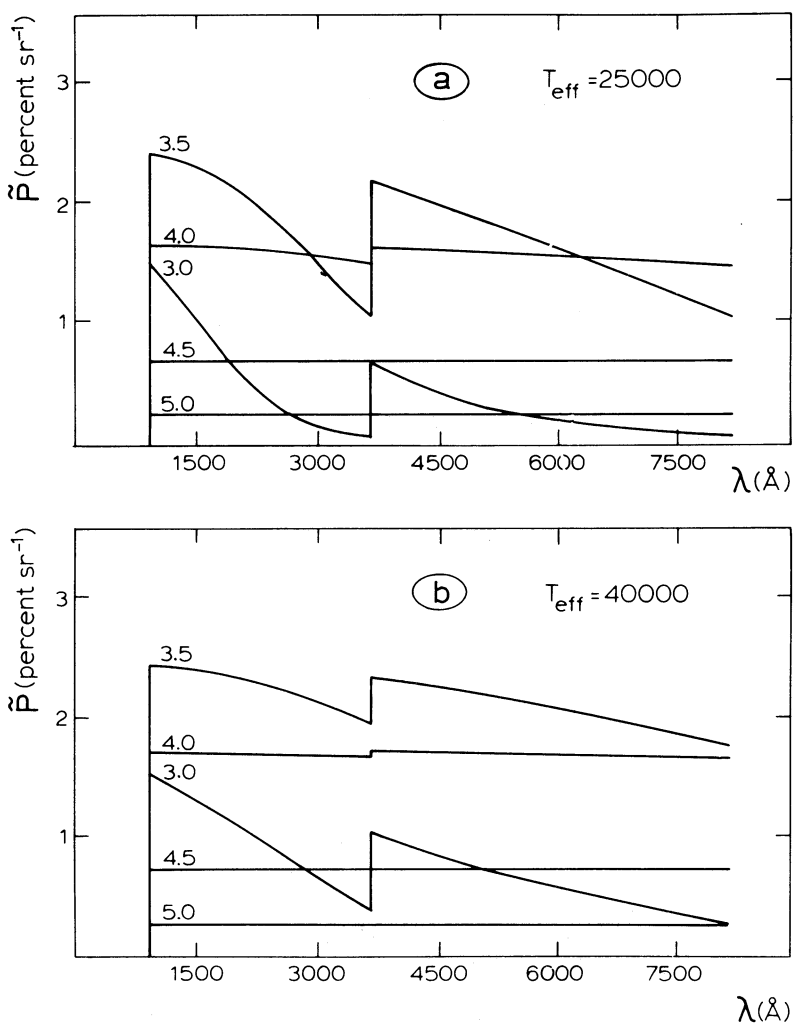

FIG. 2.—Wavelength dependence of $dP_\lambda/d\Omega$ for a hot star and a cooler star. The various distributions are labeled by the plume mass-loss parameter $\dot{M}$. Note that for the hotter star the slope of the Balmer continuum becomes steep for larger values of $\dot{M}$ than is the case for the cooler stars. This is because a relatively low fraction of hydrogen nuclei have electrons in the $n = 2$ level.

© American Astronomical Society • Provided by the NASA Astrophysics Data System

1987ApJ...317..290C

radiation mean intensity in the lines is calculated using the Sobolev escape probability factor $\beta(r)$ that depends on the velocity gradient through the wind. The method is not completely valid for the case of a plume geometry, but the approach should be an improvement over the assumption of LTE populations used in several polarization studies. We assume that the star radiates as a blackbody with $I_\nu^* = B_\nu(T_{\rm eff})$.

Figure 2 shows the wavelength dependence of polarization for stars of two temperatures: 25,000 and 40,000 K. The polarization per unit plume solid angle can reach values above 2% $\rm sr^{-1}$, and there can be a noticeable wavelength dependence, with a decrease occurring in going from long to short wavelengths across the Balmer edge. Each curve is labeled by $-(\log \dot{M})$. For the smaller mass-loss rates ($\dot{M} < 10^{-4}\ M_\odot\ \rm yr^{-1}$), the polarization is essentially wavelength independent. In comparing the results for the hotter star with the cooler one, note that the wavelength dependence is stronger in the cooler star at the same mass-loss rate. This is simply because more of the hydrogen in the plume is neutral, and thus the absorptive opacity is larger.

There are several factors that influence the wavelength dependence of the polarization that we have introduced in § III. Figure 3 shows the Balmer population parameter $\bar{q}_2$ and a Paschen population parameter $\bar{q}_3$. Using the populations derived as described above, we have computed the value of $\bar{q}_2$ using equation (36) and $\bar{q}_3$ using the corresponding equation for the $n = 3$ population, as a function of stellar temperature and mass-loss rate. Note that $\bar{q}_2$ and $\bar{q}_3$ decrease rather strongly with $T_{\rm eff}$, again because of the decreasing proportion of neutral hydrogen. Thus we expect a more pronounced wavelength dependence of the polarization in cooler early-type stars.

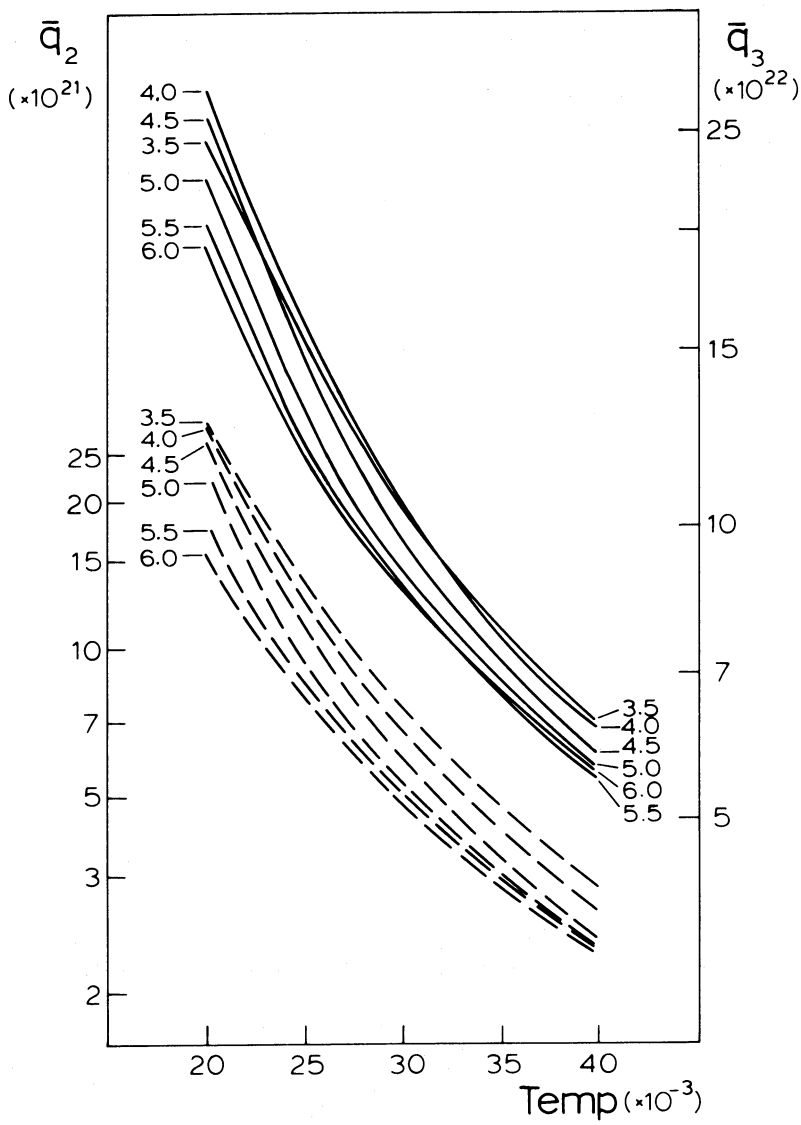

FIG. 3.—Temperature dependence of the $n = 2$ and $n = 3$ population parameters, $\bar{q}_2$ (*dashed lines*) and $\bar{q}_3$ (*solid lines*) for various mass-loss rates ($\dot{M}_* = 4\pi\dot{M}_{\rm plume}/\Omega_{\rm plume}$). Individual curves are for values $-\log(\dot{M}_*/M_\odot)$ as labeled. Note that $\bar{q}_2$ ranges from values of 3×10^{-21}, for very hot stars, up to $\sim 22 \times 10^{-21}$, for early B stars ($T \approx 20{,}000$ K).

© American Astronomical Society • Provided by the NASA Astrophysics Data System

1987ApJ...317..290C

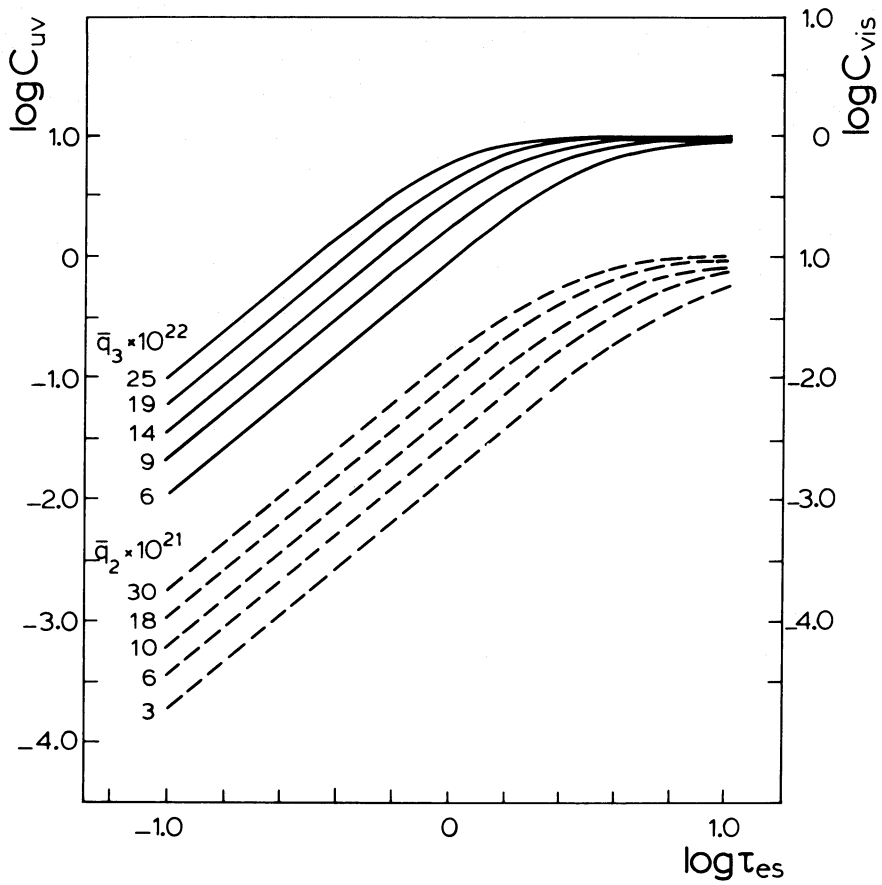

FIG. 4.—Dependence of the slope of the polarization in the Balmer continuum (or "color") on the total electron scattering optical depth in a plume. Each curve is labeled with a value for the $n = 2$ and $n = 3$ population parameters, $\bar{q}_2$ and $\bar{q}_3$. Note that the "color" is proportional to $\bar{q}$ and to the square of the electron-scattering optical depth.

To describe the slope of the polarization in the Balmer continuum we use 0.30 μm and 0.15 μm as reference wavelengths. For the Paschen continuum we use 0.44 μm and 0.7 μm. Thus the UV and optical color parameters are

$$C_{\rm UV} = \frac{P(0.15) - P(0.30)}{P(0.15)}, \qquad C_{\rm Vis} = \frac{P(0.44) - P(0.70)}{P(0.44)}. \tag{44}$$

As is shown in Figure 4, for plume optical depths of about unity and less, log C rises linearly with log $\tau_{\rm es}$ with a slope of 2. This dependence of color on the square of the electron-scattering optical depth arises because the populations of the excited levels of hydrogen tend to be proportional to n_e^2, as we described in regard to equation (35).

Figure 4 can be considered an observational diagnostic diagram. The observations provide the color C, knowledge of the star's effective temperature provides an indication of $\bar{q}$ from Figure 3, and thus we can read off the plume optical depth from Figure 4. This we call τ_c, for color-derived optical depth. Note that τ_c is independent of the narrow plume geometry parameters such as opening angle θ_p and the aspect angle i.

Now let us consider the magnitude of the polarization at some given wavelength (say $\lambda = 1500$ Å). Shown in Figure 5 is the percent polarization per unit plume solid angle, $\tilde{P}$, versus the plume optical depth for a variety of $\bar{q}_2$ values. The figure shows that the maximum value of $\tilde{P}$ is $\sim 2.5\%$ sr^{-1} (times $\sin^2 i$). The polarization rises linearly with optical depth at small τ. The effects of absorption in the plume are seen to be important in reducing the polarization only for optical depths approaching unity and above. Thus, the observed magnitude of the polarization at any wavelength is primarily a product of the total colum density, the plume solid angle and the plume inclination angle. We see that the magnitude of the polarization and the color of the polarization are two separate sources of information concerning plume structure.

Let us now isolate the quantities that affect the magnitude of the polarization. Consider the effect of the finite disk factor, D. Figure 6 shows the polarization per steradian as a function of plume optical depth both for a point source and for a star with a finite disk. The finite disk factor reduces the maximum value of $\tilde{P}$ from $\sim 6\%$ sr^{-1} to $\sim 2.5\%$ sr^{-1}. The reason for the reduction is illustrated in Figure 7. This shows the contribution to the polarization by electrons at various distances from the star, that is, the integrand of the following expression

$$\tilde{P}_\nu = \int_R^\infty \left(\frac{d^2 P_\nu}{dr d\Omega}\right) dr . \tag{45}$$

© American Astronomical Society • Provided by the NASA Astrophysics Data System

1987ApJ...317..290C

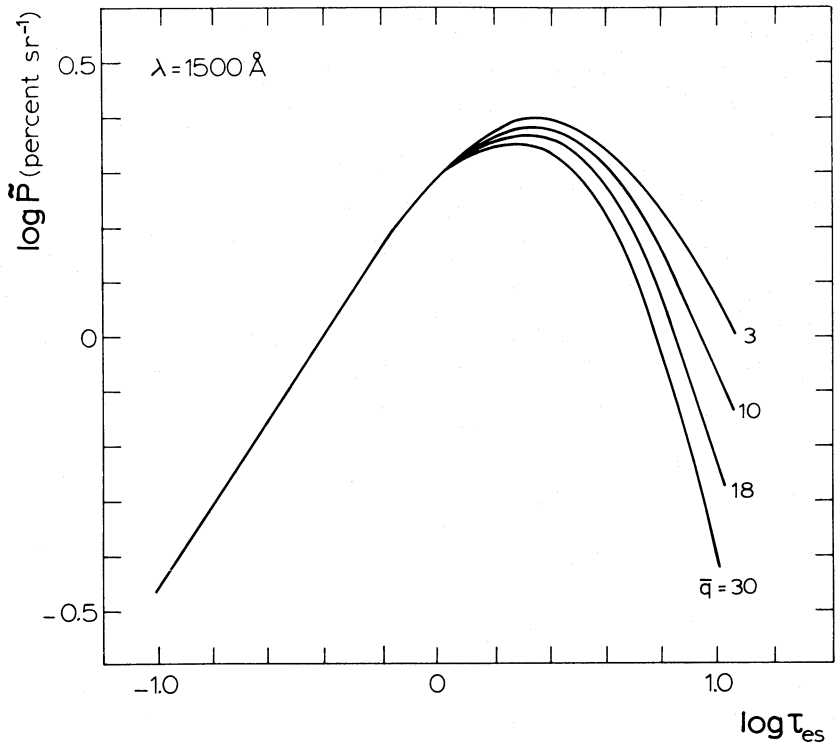

FIG. 5.—The 1500 Å polarization vs plume electron-scattering optical depth. For optical depths less than unity there is little dependence on the $n = 2$ population parameter $\bar{q}_2$ that labels each curve on the right.

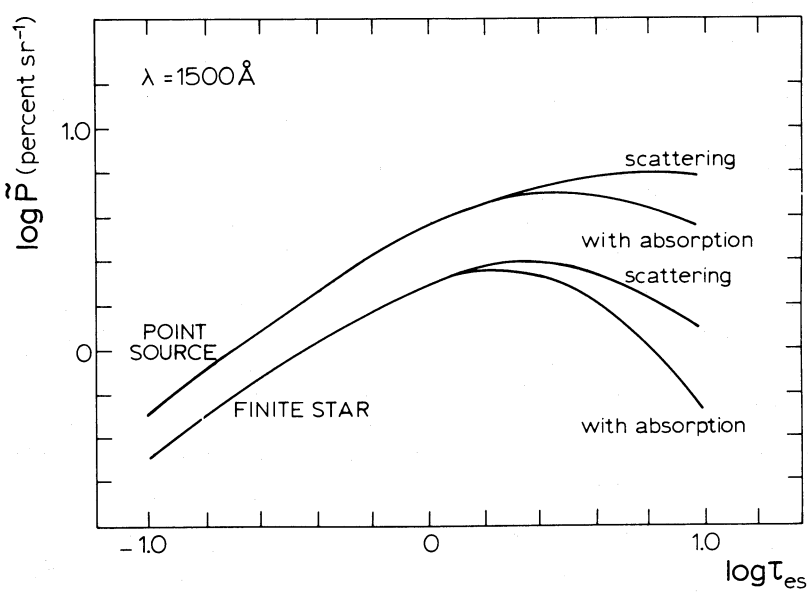

FIG. 6.—Shows the monochromatic polarization vs, electron-scattering optical depth, and illustrates the effects of absorption in the plume and of the finite disk factor. Top pair of curves are for a point source star, with scattering only occurring in the plume, and with both scattering and absorption occurring. Bottom pair of curves is for a finite-sized star in which the depolarization factor $D(r)$ is accounted for. Absorptive cases use $\bar{q}_2(T_{\rm eff}) = 18$. The lower most curve is identical to the $\bar{q}_2 = 18$ in Fig. 5.

© American Astronomical Society • Provided by the NASA Astrophysics Data System

1987ApJ...317..290C

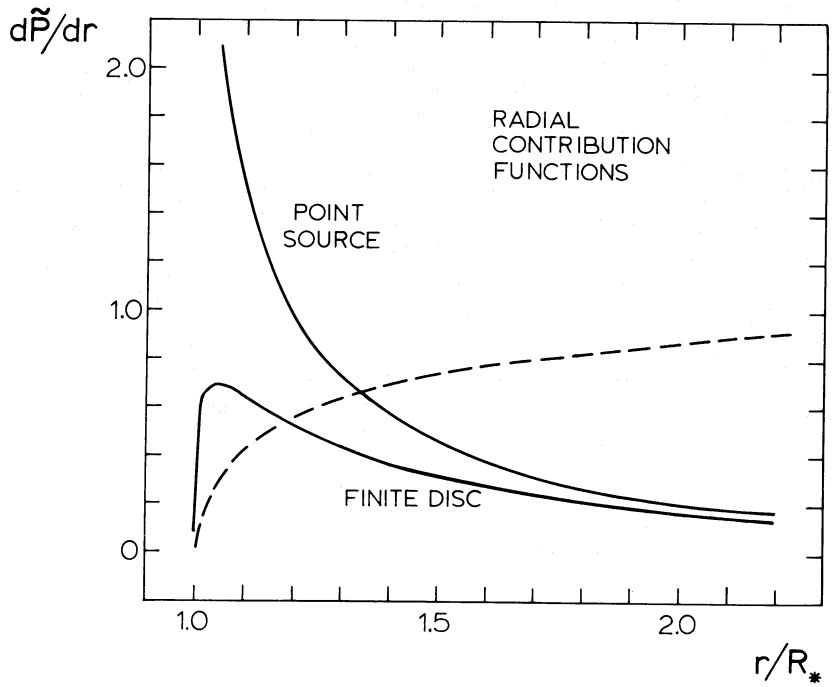

FIG. 7.—Plotted with the dashed line is the finite star correction factor $D(r)$. The radial contribution function $d^2P/drd\Omega$, both with and without the finite star correction factor, is also shown. Note the substantial effect of $D(r)$ on the polarization contribution from material near the stellar surface, where the point source contribution function has its largest value.

From equation (25) we see that

$$\frac{d^2P_\nu}{drd\Omega} \propto n_e(r)D(r)e^{-\tau}\nu \ . \tag{46}$$

The disk factor D is very small near the stellar surface, as is shown by the dashed line in Figure 7. This drastically reduces the polarization from regions near the base of the disk as is illustrated. In combination with the attenuation factor $e^{-\tau}\nu$, it leads to the decline in $\tilde{P}$ at large optical depth seen in Figure 6. The attenuation simply prevents the radiation from reaching the outer portions of the plume where the scattering is more efficient in producing polarized light. The same type of decrease with τ_{es} even occurs for the point source case when absorptive opacity is included (Fig. 6). In this case not all of the stellar radiation entering the base of the plume is scattered. We see that for the case of scattering alone the value of $\tilde{P}$ reaches an asymptotic limit of $\sim 6\%$ sr^{-1}. This asymptotic value can be derived from the ratio of the maximum polarized intensity to the total intensity from the star plus envelope. If we assume roughly that the light in the plume is scattered by 90° toward the observer, then all of the light entering the base of the plume of opening angle $\Delta\Omega$ contributes to fully polarized light (100% polarization), so the maximum polarized intensity is $L\Delta\Omega/4\pi$. The total star plus envelope intensity is $(L/4\pi)(1 + \Delta\Omega/4\pi)$, so the polarization per unit solid angle is $\tilde{P} = (4\pi)^{-1}/[1 + (4\pi)^{-1}]$, or $\sim 7.3\%$ sr^{-1}. This is slightly above the 6% sr^{-1} actually calculated because in the actual case the light scattered from the sides of the plume nearest and farthest from the observer is not quite 100% polarized.

V. SUMMARY

We have rederived the useful polarization equations of Brown and McLean (1977) for an axisymmetric distribution of electrons about a star. In this derivation we have used the formal polarization source functions of Chandrasekhar (1950) and thereby have made clearer the close relationship that exists between the Brown and McLean (1977) formulation and the earlier transfer equation methods of Cassinelli and Hummer (1972).

We have focused attention on the polarization that can arise at ultraviolet wavelengths for concentrations of wind material in plumes. There already exists evidence that flow can be concentrated in this way because of surface magnetic fields or surface nonradial pulsation. Also such concentration of mass flux can occur in many systems containing a compact companion, as has been shown by Friend and Castor (1982). Recently Friend and Cassinelli (1986) have applied the methods developed in this paper to an analysis of the Cyg X-1 system and have found that the "focused" wind picture can explain the observed magnitude of the polarization.

Throughout we have attempted to follow the approach of Brown and McLean (1977) in isolating the causes of the polarization and the wavelength dependence of the polarization. In particular, we have introduced the concept of "color of polarization" and have shown that it provides different information than is contained in the magnitude of the monochromatic polarization. In particular, the color depends on the integral of n_e^2 along the plume, while the magnitude P_λ depends on the integral of n_e. Using this property we have discussed several plots that should be useful in interpreting polarization observations at optical and ultraviolet wavelengths.

© American Astronomical Society • Provided by the NASA Astrophysics Data System

1987ApJ...317..290C

We are grateful to David Friend, Rens Waters, John Brown, and Vivette Carlaw for helpful discussions and comments. This work was supported by NASA grant NAGW-422 and was completed while J. P. C. held a Fulbright fellowship at the University of Utrecht. J. P. C. is grateful to Tony Hearn for making the visit possible.

REFERENCES

Barker, P. K., Brown, D. N., Bolton, C. T., and Landstreet, J. D. 1982, in *Advances in UV Astronomy: Four Years of IUE Research*, ed. Y. Kondo, J. M. Mead, and R. D. Chapman (NASA Conf. Pub. 2283), p. 589.
Brown, D. N., Shore, S. N., and Sonneborn, G. 1985, *A.J.*, **90**, 1354.
Brown, J. C., and McLean, I. S. 1977, *Astr. Ap.*, **57**, 141.
Capps, R. W., Coyne, G. V., and Dyck, H. M. 1973, *Ap. J.*, **184**, 173.
Cassinelli, J. P. 1985, in *The Origin of Nonradiative Heating/Momentum in Hot Stars*, ed. A. B. Underhill and A. G. Michalitsianos (NASA Conf. Pub. 2358), p. 2.
Cassinelli, J. P., and Hummer, D. G. 1971, *M.N.R.A.S.*, **154**, 9.
Cassinelli, J. P., and Olson, G. L. 1979, *Ap. J.*, **229**, 304.
Cassinelli, J. P., Olson, G. L., and Stalio, R. 1978, *Ap. J.*, **220**, 573.
Cassinelli, J. P., and Swank, J. H. 1983, *Ap. J.*, **271**, 681.
Castor, J. I. 1970, *M.N.R.A.S.*, **149**, 111.
Chandrasekhar, S. 1950, *Radiative Transfer* (London: Oxford University Press).
Collins, G. W. 1972, *Ap. J.*, **175**, 147.
Friend, D. B., and Cassinelli, J. P. 1986, *Ap. J.*, **303**, 292.
Friend, D. B., and Castor, J. J. 1982, *Ap. J.*, **261**, 293.
Haisch, B. M., and Cassinelli, J. P. 1976, *Ap. J.*, **208**, 253.
Hummer, D. G., and Rybicki, G. B. 1971, *M.N.R.A.S.*, **152**, 1.
Lupie, O. L., and Nordsieck, K. H. 1986, *A.J.*, **92**, 214.
McLean, I. S. 1979, *M.N.R.A.S.*, **186**, 265.
Mullan, D. J. 1984. *Ap. J.*, **283**, 303.
Serkowski, K. 1970, *Ap. J.*, **160**, 1083.
Shakhovskoi, N. M. 1965, *Soviet Astr.—A.J.*, **8**, 833.
Underhill, A. B. 1984, *Ap. J.*, **276**, 583.
Vogt, S. S., and Penrod, G. D. 1983, *Ap. J.*, **275**, 661.
Waters, L. B. F. M., and Cassinelli, J. P. 1987, in preparation.

J. P. Cassinelli, M. A. Murison, and K. H. Nordsieck: Astronomy Department, University of Wisconsin, 475 N. Charter Street, Madison, WI 53706

© American Astronomical Society • Provided by the NASA Astrophysics Data System